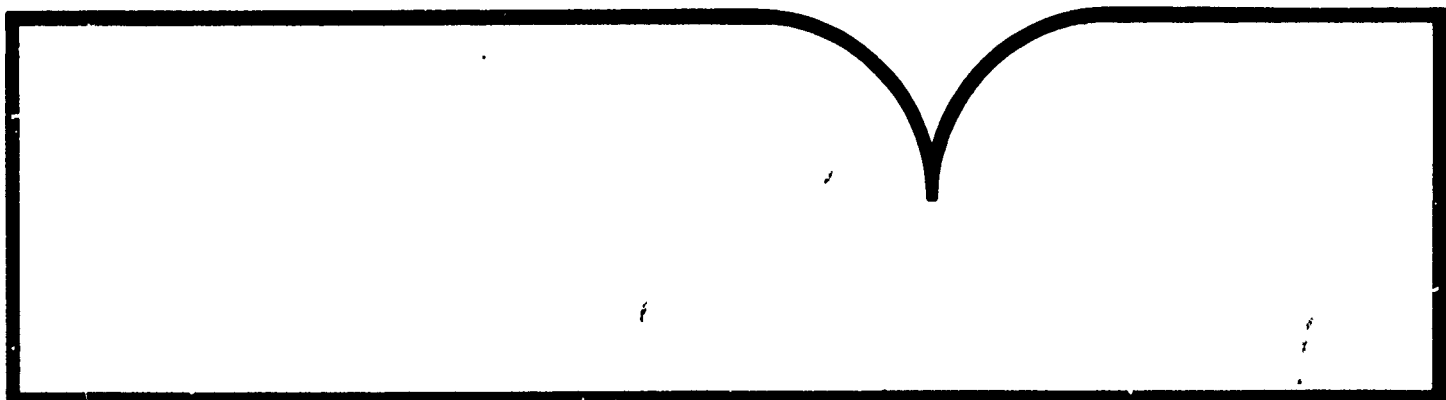


OPTICAL PROCESSING OF ULTRASONIC WAVES

Department Of Mechanical Engineering
Houston, TX

79



AD-A105929

Final Report

to the

Office of Naval Research
Contract: N00014-80-C-0591

*submitted:
(June 1981)*

OPTICAL PROCESSING OF ULTRASONIC WAVES

submitted by

Copy available to DTIC does not
permit fully legible reproduction

Bill D. Cook
Department of Mechanical Engineering
Cullen College of Engineering
University of Houston Central Campus
Houston, Texas 77004

REPRODUCED BY
NATIONAL TECHNICAL
INFORMATION SERVICE
US DEPARTMENT OF COMMERCE
SPRINGFIELD, VA. 22161

This document has been approved
for public release and sale; its
distribution is unlimited.

DISCLAIMER NOTICE

**THIS DOCUMENT IS BEST QUALITY
PRACTICABLE. THE COPY FURNISHED
TO DTIC CONTAINED A SIGNIFICANT
NUMBER OF PAGES WHICH DO NOT
REPRODUCE LEGIBLY.**

During the year prior to the contract with ONR, the principal investigator had a similar contract. During that year the principal investigator had developed the theory and algorithms of the prediction of the scattering of light by sound and the inversion procedure of investigating the sound fields from the scattered optical data. For the purpose of this report, these theories will be known as the direct theory and the inversion theory.

During the Spring of 1980, the principal investigator trained two students, Mr. Charles Fray and Mr. John R. Laflin in the aspects of acousto-optic interaction.

The objective of this contract was to allow the principal investigator and his graduate students to work with colleagues in the Physical Acoustics Branch of the Naval Research Laboratory, Washington, DC to implement algorithms on their computer data acquisition system.

During the stay at NRL, Mr. Fray, in conjunction with others, developed a modelling system which would predict the colored schlieren patterns of ultrasonic fields. The output of this model was by colored television display of computed values. The work of Mr. Fray will be continued by those at NRL.



Mr. Laflin pursued the inversion problem. That is, he developed a computer based experimental system to acquire acousto-optic data and process it to reveal the complicated near field of an ultrasonic transducer.

The principal investigator directed the students, collaborated on a new theory for tomographic processing acousto-optic data, and generally supported the Physical Acoustic Branch with theory and concepts in acousto-optics and scattering of sound.

During the extension period of the contract from September 1980 to May 1981, substantial progress has been made in the graphic routines associated with both the direct theory and inversion theory.

Attachment A is a preprint of a manuscript resulting from the tomographic work which was presented to the Acoustic Imaging conferences, Monterey, CA, Spring 1981. Attachment B and C are abstracts of papers presented at the Fall 1980 meeting of the Acoustical Society of America, Los Angeles, CA.

PLATINUM PUBLISHERS CORPORATION
227 West 17th Street
New York, N.Y. 10011

6 1/2 X 9 7/8

EVEN	REVIEWER HEAD	OPS
1		1
2		2
3	FIRST LINE OF TEXT (OTHER THAN FIRST PAGE)	3
4		4
5		5
6		6
7		7
8		8
9		9
10		10
11	TOMOGRAPHIC EVALUATION OF SOUND FIELDS	11
12		12
13	FROM ACOUSTO-OPTIC DATA	13
14		14
15		15
16	BILL D. Cook* and John F. Laflin*	16
17		17
18	Department of Mechanical Engineering	18
19	University of Houston, Houston, Texas 77004	19
20		20
21		21
22	Charles E. Gaumond and Henry D. Dardy	22
23		23
24	U.S. Naval Research Laboratory	24
25	Washington, D.C. 20375	25
26		26
27		27
28	ABSTRACT	28
29		29
30	The principles of computerized transverse tomography can be	30
31	applied to the acousto-optic reconstruction of the local sound	31
32	pressure of an ultrasonic field. For sufficiently narrow beams	32
33	of ultrasound in the low megahertz region, the total optical	33
34	phase retardation of an interrogating light beam can be consi-	34
35	dered as a projection of the sound field pressure. (Fourier	35
36	techniques for the numerical reconstruction of the pressure field	36
37	yield as intermediate steps a Fourier domain associated with the	37
38	angular spectrum of plane waves comprising the sound field.) Con-	38
39	sequently the sound field can be reconstructed in other regions	39
40	than the plane of interrogation. In this work we discuss two al-	40
41	ternative methods for acquiring data. One method builds the	41
42	Fourier domain along radial spokes which is inconvenient for	42
43	numerical processing by DFFT algorithms. The other procedure bu-	43
44	ilds the Fourier domain in a nearly rectangular format compatible	44
45	with two-dimensional DFFT algorithms. With this latter method,	45
46	it is possible to evaluate the pressure along a line with limited	46
47	data and a one-dimensional DFFT.	47
48		48
49	* Work supported in part by Physical Acoustics Center Program at	49
50	the Naval Research Laboratory, Code 5130, Washington, D.C.	50
51	20375.	51
52		52

1	EVEN	RUNNING HEAD	ODD
2			1
3	1.0 INTRODUCTION		2
4	A sound field of low ultrasonic power, low ultrasonic fre-		3
5	frequency, and narrow beam width behaves as an optical phase grat-		4
6	ing. Collimated light passing through such a sound field experi-		5
7	ences an optical phase retardation proportional to the local		6
8	sound pressure, integrated over the light path. This constitutes		7
9	a "projection" of the sound field and numerical methods of compu-		8
10	terized transverse tomography can be applied to estimate the		9
11	local sound pressure.		10
12			11
13			12
14	Numerical techniques using Fourier transforms are useful in		13
15	pressure field evaluation since an intermediate step yields the		14
16	Fourier domain associated with the angular spectrum of plane		15
17	waves comprising the sound field. Moreover, by modification of		16
18	the phase terms of each plane wave of the angular spectrum, it is		17
19	possible to construct the sound field at different planes. In		18
20	other words, an estimate of most of the sound field can be com-		19
21	puted from a set of acousto-optic data taken over a single		20
22	transverse plane. The total field, however, cannot be construct-		21
23	ed everywhere since evanescent waves near the sound source are		22
24	not accounted for. This total field concept is valid when the		23
25	sound field can be described by the Helmholtz equation, thus el-		24
26	iminating application to non-linear or highly attenuated sound		25
27	fields.		26
28			27
29	In a series of papers ¹⁻³ directed toward transducer cali-		28
30	bration Cook and Berlinghieri have described one method of data		29
31	collection which we will call Method A. Acousto-optic data is		30
32	collected at the terminus of the light paths as shown in Figure		31
33	1. These light paths are parallel to each other and are in a		32
34	plane parallel to the surface of the transducer. Sufficient data		33
35	can be acquired from interrogation of the field in one direction		34
36	if the field is symmetric. If the field is not symmetric, Method		35
37	A involves rotation of the transducer about an axis normal to the		36
38	transducer surface, such as CC'.		37
39			38
40	Here, we present an alternative method of data collection		39
41	which we will call Method B. In Method B the transducer is ro-		40
42	tated about a line AA' parallel to the transducer surface and lo-		41
43	cated in the plane of the light paths. The line AA' is also per-		42
44	pendicular to the light paths.		43
45			44
46	We will demonstrate how both methods allow the generation of		45
47	data in the angular spectrum (plane wave decomposition) domain		46
48	with both phase and amplitude information to allow evaluation of		47
49	the pressure field at the plane of measurement using Fourier		48
50	transforms.		49
51			50
52			51
53			52

PILGRIM PUBLICATIONS CORPORATION
227 West 17th Street
New York, N.Y. 10011

6 1/2 X 9 7/8

3

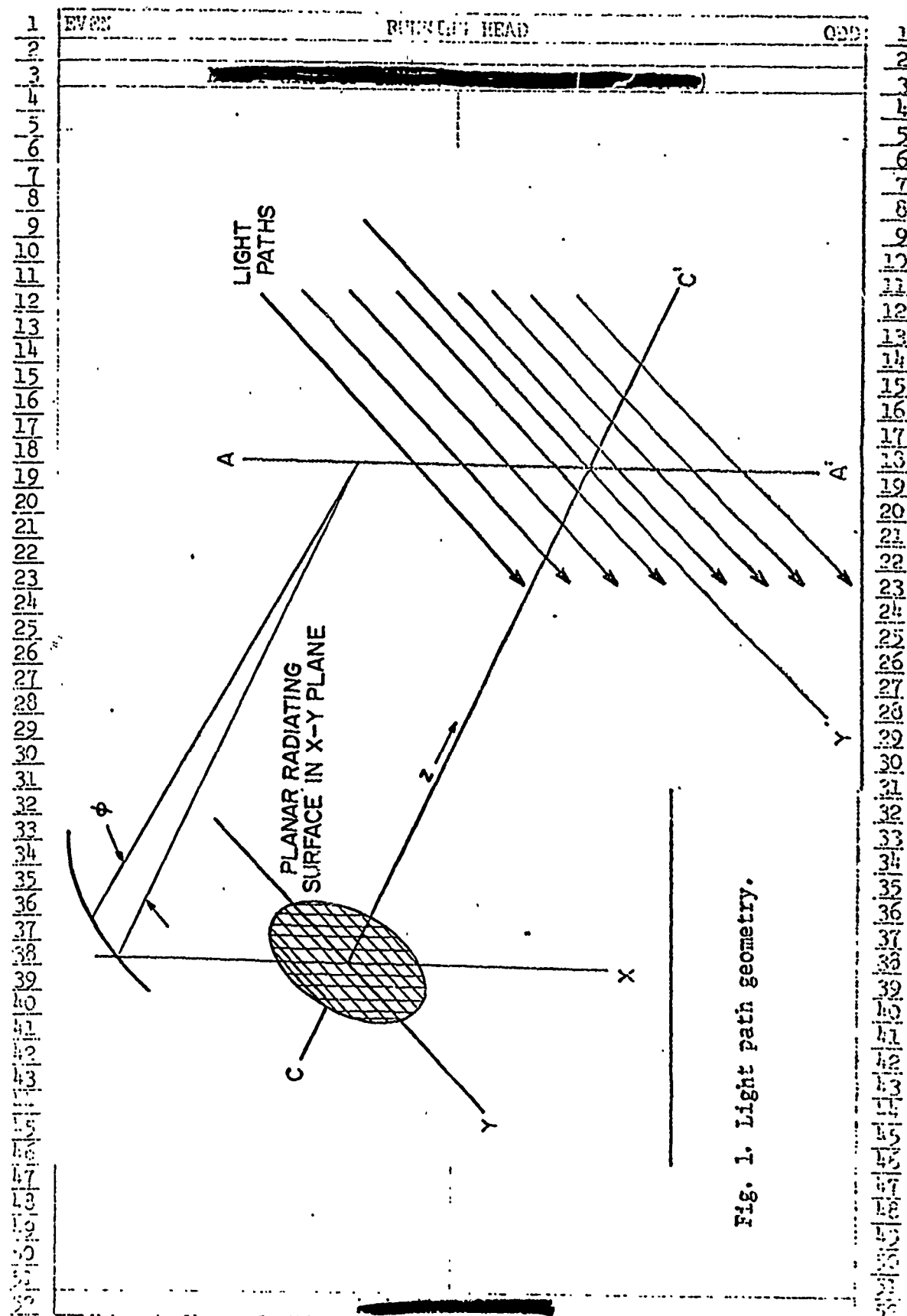


Fig. 1. Light path geometry.

1	EVEN	RUNNING HEAD	ODD
2			4
3	Data acquired using Method A builds the angular spectrum do-		3
4	main in a polar format through a series of one-dimensional Four-		4
5	ier transforms. The pressure field at the plane of measurement		5
6	can then be obtained by a two-dimensional inverse Fourier trans-		6
7	form. DFFT algorithms, however, require data to be in a rectan-		7
8	gular format. Two alternatives are to interpolate the rectangu-		8
9	lar data from the polar data or to perform a Hankel		9
10	(Fourier-Bessel) transform. The polar data becomes less dense		10
11	away from the origin so interpolation becomes questionable		11
12	there. On the other hand, development of efficient algorithms		12
13	for Hankel Transforms is now an active area of research. ⁴⁻⁶		13
14			14
15	Method B exhibits three attractive features. The first is		15
16	that through a series of one-dimensional transforms the angular		16
17	spectrum domain can be built in a format which closely approxi-		17
18	mates a rectangular raster. ¹⁰ The second feature is that the data		18
19	collected by this method lies midway between the angular spectrum		19
20	domain and the time-space domain. Evaluation of the pressure		20
21	field at the plane of measurement, therefore, requires only a		21
22	series of inverse, one-dimensional transforms. A third feature		22
23	is that acoustic pressure can be computed along a line transverse		23
24	to the direction of sound propagation by a single inverse		24
25	one-dimensional transform.		25
26			26
27			27
28	2.0 THEORY OF METHOD A		28
29			29
30	Consider a harmonic sound field being produced by a planar		30
31	transducer. Let the pressure at a distance z from the transducer		31
32	be expressed as		32
33			33
34			34
35	$p(x,y,z,t) = \tilde{p}(x,y,z)\exp(-j\omega t)$	(1)	35
36			36
37			37
38	In the following discussion the time variance will be dropped for		38
39	convenience.		39
40			40
41	Line integrals across the pressure field at $z+z_0$ can be		41
42	written		42
43			43
44			44
45	$\tilde{p}(x,z_0) = \int \tilde{p}(x,y,z_0)dy$	(2)	45
46			46
47			47
48	where the limits of this integral and others are taken from minus		48
49	infinity to plus infinity. $\tilde{p}(x,z_0)$ can be seen as a "projection"		49
50	of the pressure field $\tilde{p}(x,y,z_0)$.		50
51			51
52			52

6 1/2 X 9 7/8

1	EVEN	RUNNING HEAD	CDD
2			
3		In the design of this experiment, $\tilde{p}(x, z_0)$ is obtained from	
4		measurement of the Raman-Nath parameter V defined as	
5			
6			
7		$V(x, z_0) = [2\pi k/\lambda] \tilde{p}(x, z_0)$	(3)
8			
9			
10		where λ is the optical wavelength in vacuum and k is the medium	
11		piezo-optic coefficient which relates the index of refraction to	
12		changes in acoustic pressure. This parameter V is a measure of	
13		the optical phase retardation induced by the sound field. It is	
14		a common parameter used in most theories and can be inferred from	
15		acousto-optic measurements. This parameter, in our case, is to	
16		be measured as a phasor. Various techniques for acquiring the	
17		necessary phase and amplitude information can be found in the li-	
18		terature. ⁷⁻⁸	
19			
20		We will show the relation between the projected pressure and	
21		the Fourier domain assuming $p(x, z_0)$ to be a measurable quantity.	
22		Substitution of a two-dimensional transform expression into the	
23		integral of Equation (2) gives	
24			
25			
26		$\tilde{p}(x, z_0) = \iiint \tilde{p}(k_x, k_y; z_0) \exp[j(k_x x + k_y y)] dy dk_x dk_y$	(4)
27			
28			
29		where k_x and k_y are components of the acoustic wave vector k .	
30		The integration of the y -variable can be completed yielding the	
31		Dirac- δ function $2\pi\delta(k)$. The sifting properties of the	
32		δ function upon integration over k produce the desired result	
33			
34			
35		$\tilde{p}(x, z_0) = 1/2\pi \int p(k_x, 0; z_0) \exp(jk_x x) dk_x$	(5)
36			
37			
38		This result, sometimes referred to as the "Fourier	
39		projection-slice theorem," states that the Fourier transform of a	
40		projection is a slice of the Fourier transform of the projected	
41		function. In other words, the one-dimensional transform of	
42		$\tilde{p}(x, z_0)$ produces a single line in the Fourier domain. This line	
43		lies perpendicular to the direction of the light paths, that is	
44		the line of interrogation. Consequently, if one rotates the	
45		transducer as specified for Method A in equal angular increments	
46		(essentially around the sound field axis), the projections obta-	
47		ined are related to values in the Fourier domain located along	
48		radial lines. In other words, taking a discrete one-dimensional	
49		transform of the projections $\tilde{p}(x, z_0)$ yields values shown as cir-	
50		cles in Figure 2. This result is not restricted to sound fields	
51		and is a general result of projection theory.	
52			

$6\frac{1}{2} \times 9\frac{7}{8}$

6

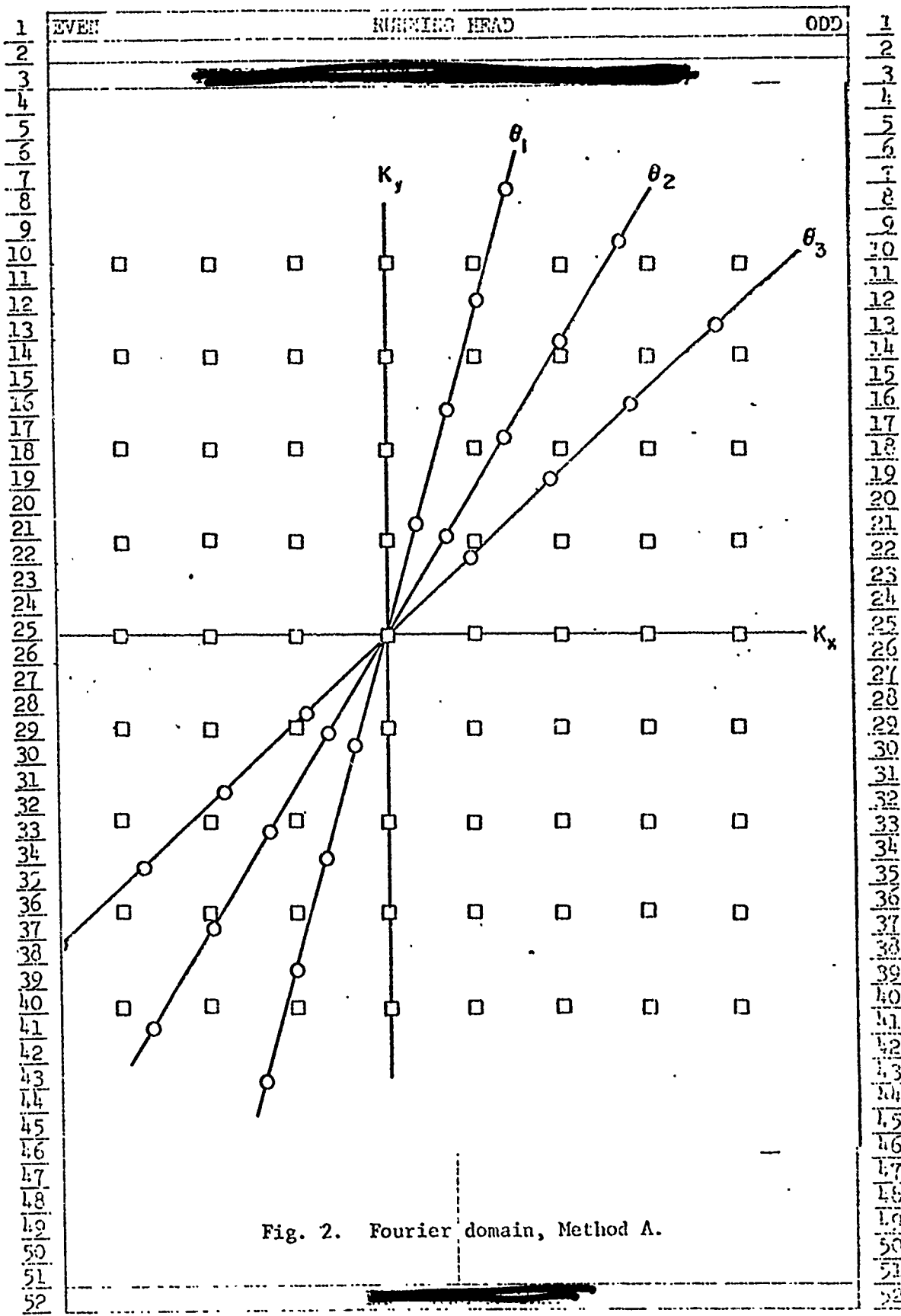


Fig. 2. Fourier domain, Method A.

1	EVEN	RUNNING HEAD	ODD
2			7
3	The previously stated difficulty is in the inversion of data		2
4	in the Fourier domain to the time-space domain from the polar		3
5	format. In addition to interpolation to a rectangular format,		4
6	Mersereau and Oppenheim suggest other schemes to circumvent this		5
7	problem. ⁹		6
8			7
9			8
10	3.0 THEORY OF METHOD B		9
11	FIRST LINE OF TITLE		10
12	Consider the origin of the (x,y,z) coordinate axes to be the		11
13	point of intersection of the acoustic axis and the plane of the		12
14	light slice. Again, z is the acoustic axis. The light path		13
15	slice will now be at an angle with the y-axis. We can write		14
16	the projection of the pressure field with the notation changed to		15
17	account for the angle as		16
18			17
19			18
20	$p(x, \phi, z) = \int \tilde{p}(x, y, z) dy'$		19
21			20
22			21
23	where dy' is along the light paths at an angle ϕ with the y-axis.		22
24			23
25	The Fourier domain pressure can be expressed as		24
26			25
27			26
28	$\tilde{p}(k_x, k_y, z) = \tilde{p}_0(k_x, k_y) \exp(jk_z z)$		27
29			28
30			29
31	where $\tilde{p}_0(k_x, k_y)$ is the Fourier component at $z = 0$ and k_z is the		30
32	z-component of the acoustic wave vector. We again substitute the		31
33	Fourier description of the pressure field in Equation (6) and in-		32
34	corporate Equation (7) to give		33
35			34
36			35
37	$\tilde{p}(x, \phi, z) = \iiint \tilde{p}_0(k_x, k_y) \exp[j(k_x x + k_y y + k_z z)] dy' dk_x dk_y$		36
38			37
39			38
40	The light path slice and the x-axis defines a new coordinate		39
41	system (x, y', z') . This is related to the (x, y, z) coordinate sys-		40
42	tem by the transformation		41
43			42
44	$y = y' \cos\phi + z' \sin\phi$		43
45	$z = -y' \sin\phi + z' \cos\phi$		44
46			45
47	Substituting this expression into Equation (8) and collecting		46
48	terms of integration of dy' , we find the integral		47
49			48
50			49
51	$\int \exp[j(k_y \cos\phi - k_z \sin\phi) y'] dy' = 2\pi \delta(k_y \cos\phi - k_z \sin\phi)$ -- (10)		50
52			51

6 1/2 X 9 1/8

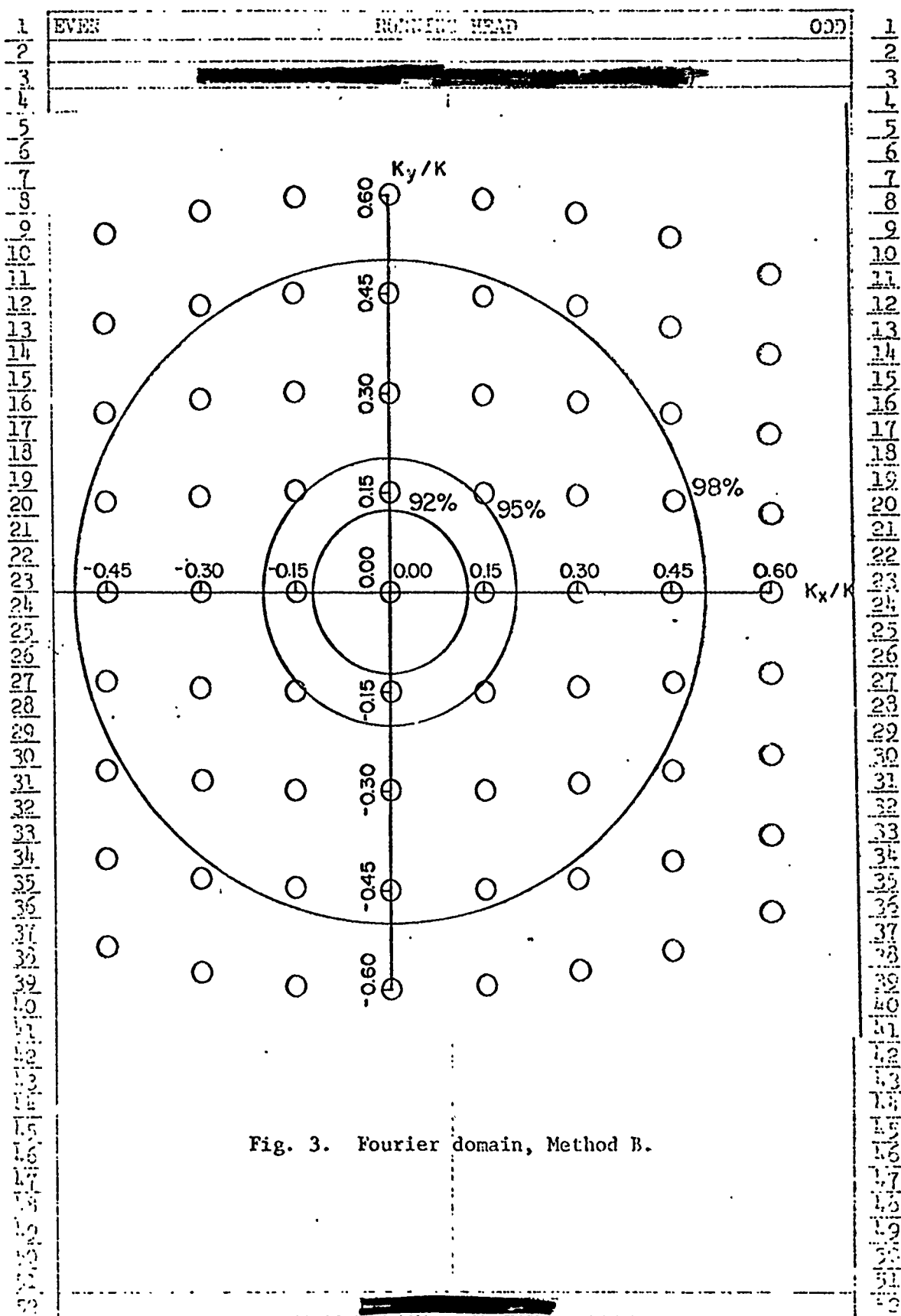
1	EVEN	ROBETING HEAD	ODD
2			
3	If we define		
4			
5		$k_y' = k_z \tan\phi$	(11)
6			
7			
8		we can write the Dirac- δ function of Equation (10) as $2\pi\delta(k_y - k_y')$. Equation (8) can now be written as	
9			
10		$\tilde{p}(x, \phi, z) = 1/2\pi \int p_0(k_x, k_y) \delta(k_y - k_y') x$	
11			
12			
13		$\exp[j(k_x x + k_y z' \sin\phi + k_z z' \cos\phi)] dk_x dk_y$	(12)
14			
15			
16			
17		The integral over dy' can be evaluated using the sifting properties of the δ function.	
18			
19		AND ADDRESS	
20			
21		$\tilde{p}(x, \phi, z) = 1/2\pi \int \tilde{p}_0(k_x, k_y') x$	
22			
23			
24		$\exp[j(k_x x + k_y' z' \sin\phi + k_z z' \cos\phi)] dk_x$	(13)
25			
26			
27		Since the origin of the coordinate system is in the plane of the light path slice, we have $z' = z_0 = 0$. Equation (13) now becomes	
28			
29			
30			
31		$\tilde{p}(x, \phi, z_0) = 1/2\pi \int \tilde{p}_0(k_x, k_y') \exp(jk_x x) dk_x$	(14)
32			
33			
34		Equation (11) can be restated as	
35			
36			
37		$k_y' = (k^2 - k_x^2) \sin\phi$	(15a)
38			
39			
40		If k_x is small compared to k , then the following approximation holds.	
41			
42			
43			
44		$k_y' = k \sin\phi$	(15b)
45			
46			
47		When this approximation is substituted into Equation (14), $\tilde{p}(x, \phi, z_0)$ becomes $\tilde{p}(x, k_y', z_0)$	
48			
49			
50			
51		$\tilde{p}(x, k_y', z_0) = 1/2\pi \int \tilde{p}_0(k_x, k_y') \exp(-jk_x x) dk_x$	(16)
52			
53			

EVEN	RUNNING HEAD	ODD
1		1
2		2
3	which is the main result of Method B.	3
4		4
5	It is important to note that $\tilde{p}(x, k_y', z_0)$ lies midway between	5
6	the Fourier domain and the time-space domain. If we take the in-	6
7	verse Fourier transform of $\tilde{p}(x, k_y', z_0)$ with respect to the vari-	7
8	able k_y' , we obtain	8
9		9
10	$\frac{1}{2\pi} \int \tilde{p}(x, k_y', z_0) \exp(jk_y' y) dk_y' =$	10
11		11
12		12
13	$(1/2\pi)^2 \iint p_o(k_x, k_y', z_0) \exp[j(k_x x + k_y' y)] dk_x dk_y' \quad (17)$	13
14		14
15	The term on the right-hand side can be recognized as $p(x, y, z_0)$.	15
16	Thus from a set of measurement taken at a given elevation (x fixed)	16
17	and varying angle, we can apply a one-dimensional Fourier	17
18	transform to obtain the pressure along the y -axis for that value	18
19	of x . The pressure over a specified $x-y$ plane can also be obtained	19
20	by a series of such transforms taken at equally spaced values of x .	20
21		21
22		22
23		23
24	If we take the Fourier transform of $\tilde{p}(x, k_y', z_0)$ with respect	24
25	to the variable x , we obtain	25
26		26
27		27
28	$\tilde{p}(k_x, k_y', z_0) = \int \tilde{p}(x, k_y', z_0) [\exp(-jk_x x)] dk_x \quad (18)$	28
29		29
30		30
31	which is the pressure field in the Fourier domain.	31
32		32
33	Implementation of Method B using DFFT algorithms requires	33
34	the approximation that k_y' does not depend on k_x . This approxi-	34
35	mation is valid when the ultrasound is confined to a narrow beam	35
36	as with sound field produced by most medical and NDE transducers.	36
37		37
38	To illustrate this approximation we show in Figure 3 the	38
39	nearly rectangular format for data obtained from Equation (16)	39
40	using an DFFT. The error incurred by assuming this format to be	40
41	rectangular will be small if most of the radiated energy is near	41
42	the origin in the Fourier domain. The illustration in Figure 3	42
43	is for a sound field produced by a circular transducer of radius	43
44	$a = 10\lambda$ where λ is the acoustic wavelength. Each of the larger	44
45	concentric circles has associated with it a percentage of total	45
46	radiated energy contained within the circle. The percentages	46
47	were calculated using an Airy pattern to approximate the sound	47
48	field. Figure 3 shows the format to be essentially rectangular	48
49	for 98% of the radiated energy in this case. Figure 4 shows the	49
50	general curve for the fraction of total energy radiated as a	50
51	function of $ka(\sin\phi)$ for the Airy function.	51
52		52
53		53

PLUMER PUBLICATIONS CORPORATION
227 West 17th Street
New York, N.Y. 10011

6 1/2 X 9 7/8

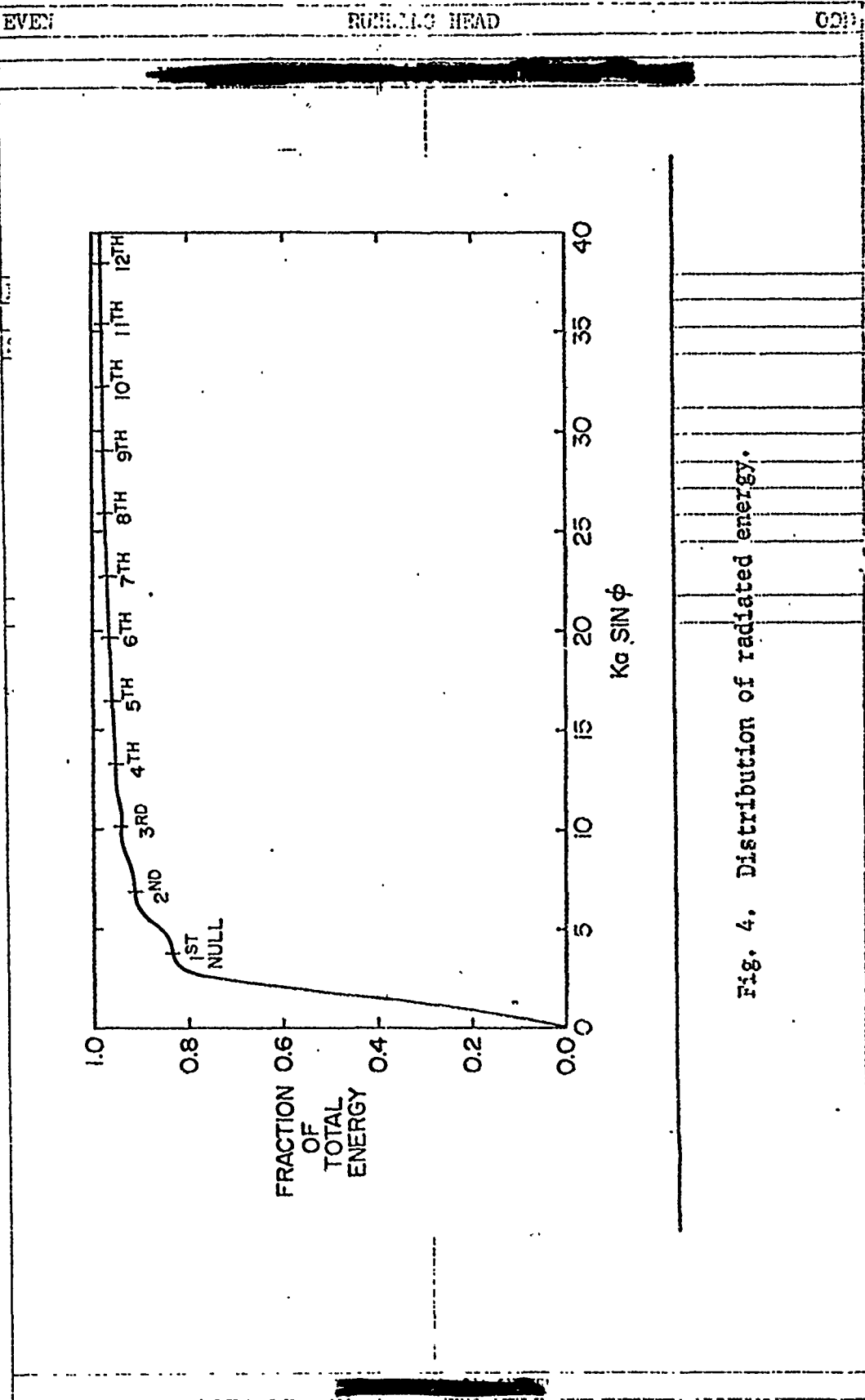
10



PLENUM PUBLISHING CORPORATION
227 West 17th Street
New York, N.Y. 10011

6 1/2 x 9 1/8

1
2
3
4
5
6
7
8
9
10
11
12
13
14
15
16
17
18
19
20
21
22
23
24
25
26
27
28
29
30
31
32
33
34
35
36
37
38
39
40
41
42
43
44
45
46
47
48
49
50
51
52
53
54
55
56
57
58
59
60
61
62
63
64
65
66
67
68
69
70
71
72
73
74
75
76
77
78
79
80
81
82
83
84
85
86
87
88
89
90
91
92
93
94
95
96
97
98
99
100



11
12
13
14
15
16
17
18
19
20
21
22
23
24
25
26
27
28
29
30
31
32
33
34
35
36
37
38
39
40
41
42
43
44
45
46
47
48
49
50
51
52
53
54
55
56
57
58
59
60
61
62
63
64
65
66
67
68
69
70
71
72
73
74
75
76
77
78
79
80
81
82
83
84
85
86
87
88
89
90
91
92
93
94
95
96
97
98
99
100

EVEN	PUNCHING HEAD	ODD
1		1
2		2
3	4.0 DATA ACQUISITION USING METHOD [REDACTED]	3
4		4
5	Equations (15a) and (15b) indicate that the angle ϕ should	5
6	change by equal increments of $\sin \phi$, or that:	6
7		7
8		8
9	$\sin \phi = +/- n\alpha$	9
10		10
11		11
12	where $n = 0, 1, 2, \dots, N$ with $2N+1$ = number of experimental points	12
13	and α = Specified increment for $\sin \phi$.	13
14		14
15	The maximum value of k_y observed in the data is	15
16		16
17		17
18	$(k_y)_{\max} = N \alpha$	18
19		19
20		20
21	From Equation (15b), we also know	21
22		22
23		23
24	$(k_y)_{\max} = k(\sin \phi_{\max})$	24
25		25
26		26
27	Combining Equations (19), (20) and (21) yields	27
28		28
29		29
30	$\Delta k_y = \alpha$	30
31		31
32		32
33	The increments of y in the transformed data returned by the	33
34	DFFT are $y = m\Delta y$ where $m = 0, 1, 2, \dots, M$ and M is the number of po-	34
35	ints used in the DFFT. From the periodicity of the DFFT, we find	35
36		36
37		37
38	$M\Delta k_y \Delta y = 2\pi$	38
39		39
40	or	40
41	$\Delta y = c/(Maf)$	41
42		42
43		43
44	where c is the sound speed, and the acoustic frequency $f = c/\lambda$.	44
45	The total range on the y -axis is then	45
46		46
47		47
48	$M\Delta y = c/(af)$	48
49		49
50		50
51		51
52		52
53		53
54		54
55		55
56		56
57		57
58		58
59		59
60		60
61		61
62		62
63		63
64		64
65		65
66		66
67		67
68		68
69		69
70		70
71		71
72		72
73		73
74		74
75		75
76		76
77		77
78		78
79		79
80		80
81		81
82		82
83		83
84		84
85		85
86		86
87		87
88		88
89		89
90		90
91		91
92		92
93		93
94		94
95		95
96		96
97		97
98		98
99		99
100		100

6 1/2 X 9 7/8

1	EVEN	READING HEAD	ODD	1
2				2
3	5.0 EXPERIMENTAL RESULTS			3
4				4
5	Cook and Berlinghieri have experimentally demonstrated the			5
6	validity of Method A. ² They generated a rectangular array of			6
7	points in the Fourier domain by rotating the transducer through			7
8	the proper angles and sampling the linear scan at proper inter-			8
9	vals. They then used a two-dimensional DFFT to reconstruct the			9
10	acoustic field in the plane of interrogation and in nearby			10
11	planes.			11
12				12
13	Method B was used to calculate the pressure distribution			13
14	over a transverse plane for a 1.25 cm. diameter PZT transducer			14
15	submersed in water. The transducer was operating at 2.2 Mhz. ($a =$			15
16	9.3λ). A total of 41 x 41 data points using a value of $\phi =$			16
17	$\sin(1 \text{ degree})$ were used to measure the pressure in a plane 5 cm.			17
18	from the transducer face. This data was used to construct the			18
19	pressure field over an area 3.9 x 3.9 cm. The results are shown			19
20	in Figure A. The effects of the approximation made in Equation			20
21	(15) are noticeable in the reconstruction. The reconstructed			21
22	field is slightly elliptical rather than circular due to the out-			22
23	ward displacement of the wave vector components in the recon-			23
24	struction.			24
25				25
26				26
27	6.0 REFERENCES			27
28				28
29	1. J. Berlinghieri and B. Cook, <u>J. Acoust. Soc. Am.</u>			29
30	<u>58</u> , 823-827 (1975).			30
31				31
32	2. B. Cook and J. Berlinghieri, <u>Proc. IEEE Ultrason. Symp.</u> <u>75</u> , CHO 944-SU, 133-135 (1975).			32
33				33
34				34
35	3. B. Cook and J. Berlinghieri, <u>J. Acoust. Soc. Am.</u>			35
36	<u>61</u> , 147-1480 (1977).			36
37				37
38	4. J. P. Clero and C. H. Durney, <u>Proc. IEEE</u> <u>67</u> , 1463			38
39	(1979).			39
40				40
41	5. Alan V. Oppenheim, G. V. Frisk, and D. R. Martinez, <u>Proc. IEEE</u> <u>66</u> , 264-265 (1978).			41
42				42
43				43
44	6. A. J. Jerri, <u>Applicable Analysis</u> <u>7</u> , 97-109 (1978).			44
45				45
46	7. Ward A. Riley, <u>J. Acoust. Soc. Am.</u> <u>65</u> , 82-85 (1979).			46
47				47
48	8. B. Cook, <u>J. Acoust. Soc. Am.</u> <u>60</u> , 95-99 (1976).			48
49				49
50	9. R. Nersereau and A. Oppenheim, <u>Proc. IEEE</u> <u>62</u> ,			50
51	1319-1338 (1974).			51
52				52

PLenum Publishers CORPORATION
227 West 17th Street
New York, N.Y. 10011

$6\frac{1}{2} \times 9\frac{7}{8}$

14

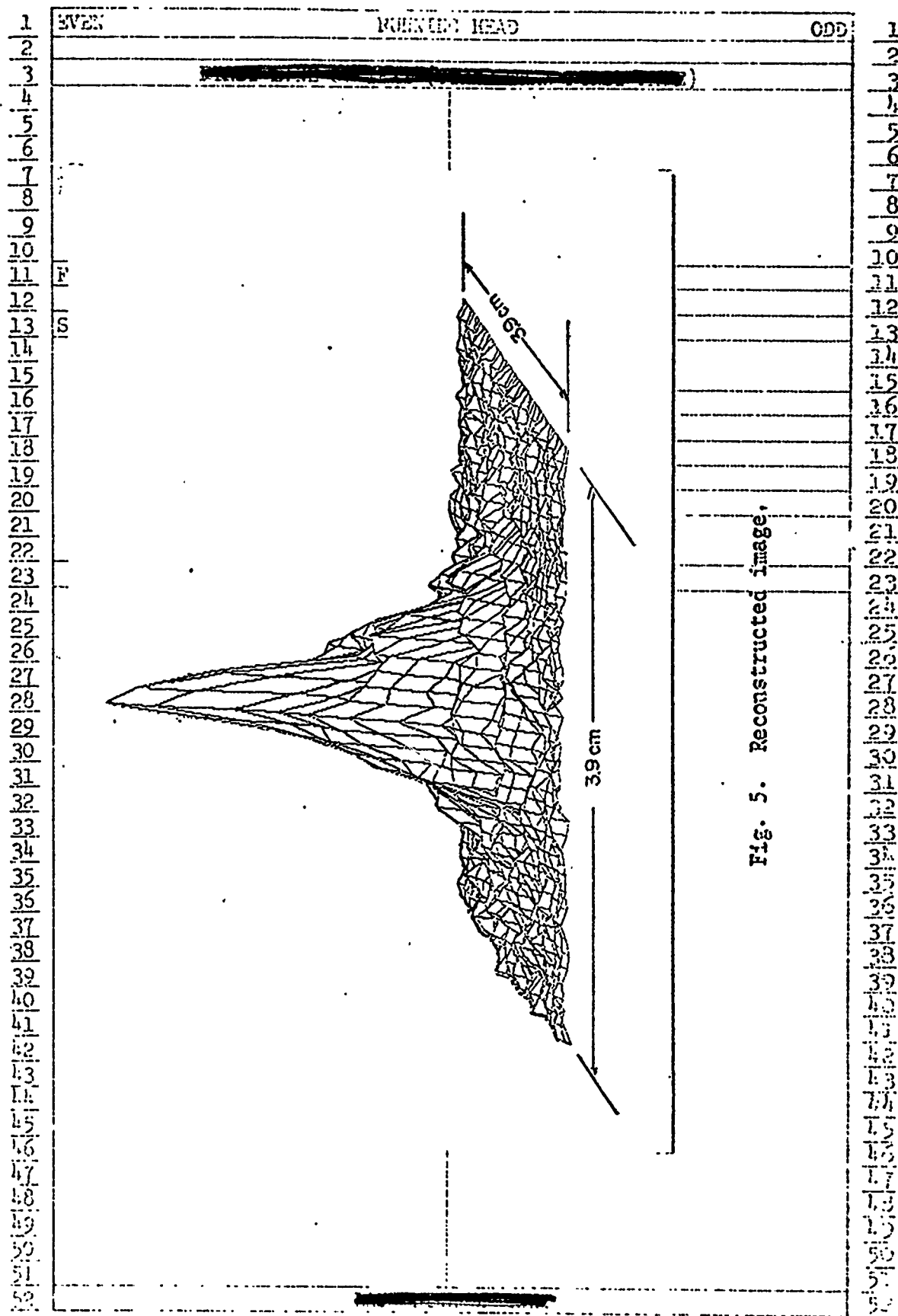


Fig. 5. Reconstructed image.